Base Hydrolysis in Homometallic Dinuclear Chromium(III) Complexes bridged by Hydroxide and Carboxylate

Takashi Fujihara,[a] Yuriko Abe[b] and Sumio Kaizaki*,[a]

[a] *Department of Chemistry, Faculty of Science, Osaka University, Toyonaka, Osaka 560, Japan*

[b] *Department of Chemistry, Faculty of Science, Nara Women's University, Nara 630, Japan*

Base hydrolysis of dinuclear complexes $[Cr_2(\mu\text{-}OH)(\mu\text{-}RCO_2)(en)_4]^{4+}$ and $[(nta)Cr(\mu\text{-}OH)(\mu\text{-}RCO_2)Cr(en)_2]^+$ (en = ethane-1,2-diamine, nta = nitrilotriacetate; R = H, Me, Et, Pr^n, CH_2Cl, CH_2ClCH_2, $MeOCH_2$ or Ph) was studied by using the UV/VIS absorption and ^2H NMR spectral changes and chromatography. The reactions were found to occur in two stages: the first-stage rates (k_1) varied with R, but the second-stage ones (k_2) were almost the same throughout the series. Analysis of the kinetic data for the two types of complexes disclosed the effects of the substituent groups R and/or the non-bridging ligands on the carboxylato bridge-cleavage reaction mechanism. Examination of the substituent effects in terms of Taft's equation with the electronic (ρ^*) and steric (δ) parameters gave a critical clue to establishing the difference in bond-cleavage sites. The values were $\rho^* = 2.29 \pm 0.20$ and $\delta = 1.41 \pm 0.13$ for $[Cr_2(\mu\text{-}OH)(\mu\text{-}RCO_2)(en)_4]^{4+}$ and $\rho^* = 0.01 \pm 0.11$ and $\delta = 0.32 \pm 0.08$ for $[(nta)Cr(\mu\text{-}OH)(\mu\text{-}RCO_2)Cr(en)_2]^+$. The carboxylato bridge-cleavage reaction is influenced by both the inductive and steric effects of the substituents in $[Cr_2(\mu\text{-}OH)(\mu\text{-}RCO_2)(en)_4]^{4+}$, and both effects contribute to smaller extents for $[(nta)Cr(\mu\text{-}OH)(\mu\text{-}RCO_2)Cr(en)_2]^+$; the former complexes undergo cleavage at the carboxylic acyl C–O bond and the latter at the Cr–O bond in the $Cr(en)_2$ site.

A number of chromium(III) dinuclear complexes have been investigated from spectroscopic and/or magnetic or kinetic viewpoints.[1–16] We have studied the electronic contribution to the magnetic interaction in dinuclear chromium(III) complexes containing bridging 4-substituted-phenols.[1] The magnetic interactions in five μ-phenoxo complexes tended to increase with increasing pK_a values of the 4-substituted-phenols or the electron density at the bridging oxygen ligators. Gafford and co-workers[2,3a] found relations between the pK_a values of carboxylic acids with the ionization constants of the bridging OH group and with the magnetic interactions in dinuclear chromium(III) complexes. On the other hand, there have been few studies on the correlation between the acid strengths of carboxylate bridging ligands and the reactivities in the bridging units. From a semiquantitative comparison of half-lives, Springborg and Toftlund[4] reported that the base hydrolysis of $[Cr_2(\mu\text{-}OH)(\mu\text{-}RCO_2)(en)_4]^{n+}$ (R = H or Me, $n = 4$; R = NH_3CH_2, $n = 5$; en = ethane-1,2-diamine) was affected by the strengths of the free carboxylic acids. A kinetic study on the CF_3CO_2-bridged complex $[Cr_2(\mu\text{-}OH)(\mu\text{-}CF_3CO_2)(en)_4]^{4+}$ also revealed that hydrolysis occurs in two stages with facile C–O bond cleavage.[5a] Recently, Tekut and Holwerda[3b] studied the influence of substituents on the aquation rate constants for acid and base hydrolysis of $[(tmpa)Cr(\mu\text{-}OH)(\mu\text{-}RCO_2)Cr(tmpa)]^{3+}$ [R = H, Me, CH_2Cl, $CHCl_2$, CMe_3, CPh_3, 1-adamantyl or 4-substituted Ph; tmpa = tris(2-pyridylmethyl)-amine].

In the course of a spectroscopic[6] and synthetic[7] study of $[(nta)Cr(\mu\text{-}OH)_2M(en)_2]^+$ (nta = nitrilotriacetate, M = Cr^{III} or Co^{III}) complexes it was found that $[(nta)Cr(\mu\text{-}OH)_2Cr(en)_2]^+$ reacts with many carboxylic acids (RCO_2H) to form $[(nta)Cr(\mu\text{-}OH)(\mu\text{-}RCO_2)Cr(en)_2]^+$. This new type of dinuclear complex is expected to become a suitable candidate to clarify in more detail the dependence of base hydrolysis on the kind of non-bridging ligand and/or carboxylate in comparison with $[Cr_2(\mu\text{-}OH)(\mu\text{-}RCO_2)(en)_4]^{4+}$.

We report here the synthesis and the kinetics of base hydrolysis of $[Cr_2(\mu\text{-}OH)(\mu\text{-}RCO_2)(en)_4]^{4+}$ and $[(nta)Cr(\mu\text{-}OH)(\mu\text{-}RCO_2)Cr(en)_2]^+$ at 25 °C (R = H, Me, Pr^n, CH_2Cl, CH_2ClCH_2, MeOCH or Ph). The base hydrolysis rates and the reaction mechanisms will be discussed to reveal the effects of the substituent group R and the dependence on the non-bridging ligand.

Experimental

Materials.—All chemicals used were analytical reagent grade. Deuteriated acetic acid with 99 atom % ^2H was obtained from Merck. The complexes *cis*-$[CrCl_2(en)_2]Cl\cdot H_2O$[14] and $K_2[Cr_2(nta)_2(\mu\text{-}OH)_2]\cdot 4H_2O$[15] were prepared according to the literature.

Preparation of the Complexes.—Δ,Λ-$[Cr_2(\mu\text{-}OH)(\mu\text{-}RCO_2)(en)_4][ClO_4]_4$. The previously reported complexes with (R = H or Me) and newly prepared complexes with R = CH_2Cl, $MeOCH_2$, Et, Pr^n or CH_2ClCH_2 were obtained from Δ,Λ-$[Cr_2(\mu\text{-}OH)_2(en)_4]^{4+}$ by the method of Springborg and Toftlund.[4]

$[(nta)Cr(\mu\text{-}OH)(\mu\text{-}RCO_2)Cr(en)_2]Cl$. All the complexes of this type (R = H, Me, CH_2Cl, $MeOCH_2$, Et, Pr^n, CH_2ClCH_2 or Ph) were synthesized by the following method. The complex *cis*-$[CrCl_2(en)_2]Cl\cdot H_2O$ (0.74 g, 2.5 mmol) was dissolved in water (20 cm^3) at 60 °C with stirring. To the resultant red solution was added $K_2[Cr_2(nta)_2(\mu\text{-}OH)_2]\cdot 4H_2O$ (0.84 g, 1.25 mmol). The mixture was stirred for 10 min, becoming a clear solution. After neutralization with 2 mol dm^{-3} NaOH solution, stirring for 30 min at 60 °C gave a violet solution. The violet complex was identified as $[(nta)Cr(\mu\text{-}OH)_2Cr(en)_2]^+$ by UV/VIS absorption spectra and elemental analysis.[7] To the violet solution was added RCO_2H (10 mmol).

The mixture was stirred at 45 °C for 20 min. The colour changed from violet to reddish violet. After cooling to room temperature, the solution was adjusted to pH 7 with 2 mol dm^{-3} NaOH solution. The filtered solution was poured onto a 3.5 × 60 cm column of SP-Sephadex (C-25, Na^+) cation exchanger. After washing with water, the charged complex was eluted with 0.1 mol dm^{-3} NaCl solution. Two bands were obtained, the second violet one (E2) being confirmed to be unreacted $[(nta)Cr(\mu\text{-}OH)_2Cr(en)_2]^+$ by its UV/VIS absorption spectrum.[7] The first reddish violet band (E1) was

condensed with a vacuum rotary evaporator to as small a volume as possible at 25 °C. A white precipitate of NaCl was filtered off. After repeated removal of NaCl in the same manner, ethanol and acetone were added to the condensed E1 eluate. The solution was allowed to stand in a refrigerator whereupon reddish violet crystals were obtained. Recrystallization was carried out by addition of ethanol and acetone to the concentrated aqueous solution, followed by standing in a refrigerator. Yield 46–58% (based on Cr).

The deuteriated complexes were synthesized by a similar method using the deuteriated nta ligand[15] and/or CD_3CO_2D.

Instruments.—The UV/VIS spectra were recorded on Hitachi 330 and Shimadzu UV-2100 spectrophotometers at room temperature. Stopped-flow measurements were carried out on an Union Giken RA-401 spectrophotometer. Hydrogen-2 NMR spectra were recorded using a JEOL JNM-GSX-270 FT spectrometer at 25 °C. The data were collected on mixing solutions initially containing equivalent volumes of 0.01 mol dm^{-3} solutions of the complexes and 1 mol dm^{-3} NaOH solution in a 10 mm tube. The external standard was C^2HCl_3 (δ 7.24), with downfield shifts defined as positive. Infrared spectra were recorded on a Shimadzu IR-435 spectrophotometer on KBr pellets. Magnetic susceptibilities were measured on powdered samples by using the Faraday method as described previously.[16] The temperature-dependent magnetic susceptibility data were fitted by the Van Vleck equation (1) defined by the

$$\chi = \frac{Ng^2\beta^2}{kT} \cdot \frac{2\exp(2J/kT) + 10\exp(6J/kT) + 8\exp(12J/kT)}{1 + 3\exp(2J/kT) + 5\exp(6J/kT) + 7\exp(12J/kT)} \quad (1)$$

exchange Hamiltonian $H = -2J(S_1 \cdot S_2)$ where $2J$ is the spin-exchange coupling constant in cm^{-1}. The coupling constants ($2J$) were derived from non-linear least-squares fits of χ to T.

Kinetic Measurements.—The kinetics of base hydrolysis for $[Cr_2(\mu\text{-}OH)(\mu\text{-}RCO_2)(en)_4]^{4+}$ were monitored at 363 and 527 nm in 10 mm quartz cells thermostatted at 25 ± 0.1 °C, using a Shimadzu UV-2100 spectrophotometer. Since the reactions of the μ-formato and μ-monochloroacetato complexes were very fast they were followed at 363 nm by employing the stopped-flow method. The hydroxide-ion concentration dependence of the rates was investigated for the reactions with NaOH solution ranging in concentration from 0.1 to 0.5 mol dm^{-3}. The initial concentration of the complexes was 3×10^{-3} mol dm^{-3}. All spectrophotometric measurements were made by mixing equivalent volumes of each solution in a cell at constant ionic strength of 0.5 mol dm^{-3} adjusted with $NaClO_4$. The pseudo-first-order rate constants for the en complexes were satisfactorily obtained from non-linear least-squares fits of $A(t)$ to t using relationship (2) where A_0, A_{inf} and $A(t)$ refer to the absorbances at the initial, infinite, and t time, respectively.

$$A(t) = A_{inf} + (A_0 - A_{inf})\exp(-k_{obs}t) \quad (2)$$

The base hydrolysis of $[(nta)Cr(\mu\text{-}OH)(\mu\text{-}RCO_2)Cr(en)_2]^+$ was followed spectrometrically by using a Shimadzu UV-160 or UV-2100 spectrophotometer at 700 nm in 10 mm quartz cells thermostatted at 25 ± 0.1 °C. The hydroxide-ion concentration dependence of the rates was investigated for reactions with NaOH solution ranging in concentration from 0.05 to 2 mol dm^{-3} at constant ionic strength of 2 mol dm^{-3} adjusted with $NaClO_4$. The initial concentration of the complexes was 5×10^{-3} mol dm^{-3}. Since the kinetics for the nta complexes is biphasic the pseudo-first-order rate constants of the two reaction steps were obtained from non-linear least-squares fits of $A(t)$ to t using equations (3a)–(3c) where ε_A, ε_B, ε_C and ε_D are the molar absorption coefficients (dm^3 mol^{-1} cm^{-1}) of

$$A(t) = A_{inf} + \alpha\exp(-k_{1obs}t) + \beta\exp(-k_{2obs}t) \quad (3a)$$

$$\alpha = \frac{(\varepsilon_A - \varepsilon_B)k_{1obs} + (\varepsilon_A - \varepsilon_C - \varepsilon_D)k_{2obs}}{k_{2obs} - k_{1obs}}[A_0] \quad (3b)$$

$$\beta = \frac{(\varepsilon_C + \varepsilon_D - \varepsilon_B)k_{1obs}}{k_{2obs} - k_{1obs}}[A_0] \quad (3c)$$

$[(nta)Cr(\mu\text{-}O)(\mu\text{-}RCO_2)Cr(en)_2]$, $[(HO)(nta)Cr(\mu\text{-}OH)Cr(en)_2(OH)]$, *cis*-$[Cr(OH)_2(en)_2]^+$ and $[Cr(nta)(OH)_2]^{2-}$, respectively and $[A_0]$ is the initial concentration (mol dm^{-3}) of the nta complexes. The observed ε_C and ε_D values (2 and 13 dm^3 mol^{-1} cm^{-1}, respectively) from the absorption spectra of the corresponding mononuclear complexes were used. The values of k_{1obs}, k_{2obs}, ε_A and ε_B were satisfactorily obtained by non-linear least-squares fits; ε_A and ε_B are comparable with those estimated from the absorption spectra.

Kinetic runs were carried out at least three times. Reactions were followed for at least four half-lives. The reproducibility of the rate constants for repeated experiments was within 9%.

Column Chromatography.—Reaction intermediates were isolated from solution by column chromatography on SP-Sephadex (C-25, NH_4^+ form, 1.5 × 20 cm) and/or QAE-Sephadex (A-25, Cl^- form, 1.5 × 20 cm). The ion-exchange resins were swelled in 0.1 mol dm^{-3} NH_3–NH_4Cl aqueous buffered solution at pH 9.5 and poured into the column. The eluting solution was 0.1–0.01 mol dm^{-3} NH_3–NH_4Cl aqueous solution.

Results and Discussion

Characterization and Stereochemistry.—For the newly prepared en and nta complexes, the satisfactory analytical data (Table 1), the UV/VIS absorption (Table 2) and IR spectra (Table 3) and/or the column chromatographic behaviour indicate carboxylate-bridged dinuclear structures. For the nta complexes, the observation of an absorption maximum (*ca.* 509 nm) and a shoulder (*ca.* 590 nm) shows the existence of the two chromophores *cis*-$[Cr(en)_2O_2]$ and $[Cr(nta)O_2]$. The separation between the asymmetric (ν_{asym}) and symmetric (ν_{sym}) IR stretching frequencies for the carboxylates in the en and nta complexes indicates carboxylate bridging ligands as shown in Table 3. These separations $\Delta\nu = \nu_{asym} - \nu_{sym}$ are smaller than those for the corresponding sodium salts. A linear correlation was found between ν_{asym} and the pK_a values for the bridging carboxylates as previously observed.[2,3a,4,17] The dinuclear structures of the nta complexes are also supported by antiferromagnetic exchange interactions ($2J$ values) which show little variation (−20.0 to −22.6 cm^{-1}, see Table 6).

Two geometrical isomers **a** and **b** are possible for $[(nta)Cr(\mu\text{-}OH)(\mu\text{-}RCO_2)Cr(en)_2]^+$. The ^2H NMR spectra of the deuteriated complex $[\{[^2H_6]nta\}Cr(\mu\text{-}OH)(\mu\text{-}CD_3CO_2)Cr(en)_2]^+$ gave three signals (δ −11.0, −24.6 and −31.5) for $[^2H_6]nta$ and one (δ 47.4) for CD_3CO_2. This indicates the existence of only one geometrical isomer, not a mixture of two. The following considerations suggest that **a** is more favoured than **b**. The complexes $[(nta)Cr(\mu\text{-}OH)(\mu\text{-}RCO_2)Cr(en)_2]^+$ are formed by the reaction of $[(nta)Cr(\mu\text{-}OH)_2Cr(en)_2]^+$ with free RCO_2H. Under the acidic conditions, hydroxide-bridge cleavage of $[(nta)Cr(\mu\text{-}OH)_2Cr(en)_2]^+$ occurs first to give $[(nta)(H_2O)Cr(\mu\text{-}OH)Cr(H_2O)(en)_2]^{2+}$ before formation of $[(nta)Cr(\mu\text{-}OH)(\mu\text{-}RCO_2)Cr(en)_2]^+$. From our X-ray crystallographic study of $[(nta)Cr(\mu\text{-}OH)_2Cr(tn)_2]^+$ (tn = propane-1,3-diamine),[7] the (nta)Cr–OH bond *cis* to the tertiary amine nitrogen in nta is longer by 0.05 Å than that *trans*. Thus, it is plausible that acid-catalysed cleavage could occur at the *cis* position to the tertiary amine nitrogen in the nta

Table 1 Analytical data for the dinuclear complexes

Compound	Found (Calc.) (%) C	H	N
$[Cr_2(OH)(EtCO_2)(en)_4][ClO_4]_4 \cdot 2H_2O$	15.45 (15.20)	4.95 (4.90)	13.05 (12.90)
$[Cr_2(OH)(Pr^nCO_2)(en)_4][ClO_4]_4 \cdot 0.5H_2O$	16.65 (16.85)	4.70 (4.85)	12.90 (13.10)
$[Cr_2(OH)(CH_2ClCO_2)(en)_4][ClO_4]_4$	14.00 (14.10)	4.30 (4.15)	12.90 (13.15)
$[Cr_2(OH)(CH_2ClCH_2CO_2)(en)_4][ClO_4]_4 \cdot 2H_2O$	14.65 (14.65)	4.60 (4.60)	12.45 (12.40)
$[Cr_2(OH)(MeOCH_2CO_2)(en)_4][ClO_4]_4 \cdot 4H_2O$	15.05 (15.25)	4.60 (4.65)	12.75 (12.95)
$[(nta)Cr(OH)(HCO_2)Cr(en)_2]Cl \cdot 4.5H_2O$	22.10 (22.35)	5.45 (5.65)	11.35 (11.85)
$[(nta)Cr(OH)(MeCO_2)Cr(en)_2]Cl \cdot 3H_2O$	25.15 (24.95)	5.70 (5.60)	11.95 (12.10)
$[(nta)Cr(OH)(EtCO_2)Cr(en)_2]Cl \cdot 2.5H_2O$	26.80 (27.00)	5.70 (5.60)	12.00 (11.90)
$[(nta)Cr(OH)(Pr^nCO_2)Cr(en)_2]Cl \cdot H_2O$	29.40 (29.50)	5.70 (5.65)	12.10 (12.30)
$[(nta)Cr(OH)(CH_2ClCO_2)Cr(en)_2]Cl \cdot 1.5H_2O$	24.25 (24.65)	4.70 (4.80)	11.45 (11.95)
$[(nta)Cr(OH)(MeOCH_2CO_2)Cr(en)_2]Cl \cdot 2H_2O$	26.00 (26.45)	5.40 (5.45)	11.65 (11.85)
$[(nta)Cr(OH)(CH_2ClCH_2CO_2)Cr(en)_2]Cl \cdot 2H_2O$	25.55 (25.65)	5.20 (5.15)	11.60 (11.50)
$[(nta)Cr(OH)(PhCO_2)Cr(en)_2]Cl \cdot 2.5H_2O$	32.45 (32.35)	5.25 (5.25)	11.10 (11.10)

Table 2 Visible absorption spectral data for $[Cr_2(\mu\text{-}OH)(\mu\text{-}RCO_2)(en)_4]^{4+}$ and $[(nta)Cr(\mu\text{-}OH)(\mu\text{-}RCO_2)Cr(en)_2]^+$ complexes

	λ_{max}/nm (ε/dm^3 mol^{-1} cm^{-1})				
	$[Cr_2(\mu\text{-}OH)(\mu\text{-}RCO_2)(en)_4]^{4+}$ [a]		$[(nta)Cr(\mu\text{-}OH)(\mu\text{-}RCO_2)Cr(en)_2]^+$ [b]		
R = H	504 (202)	376 (90)	590 (sh) (90)	509 (128)	403 (128)
Me	505 (210)	378 (99)	590 (sh) (90)	507 (141)	404 (133)
Et	505 (208)	377 (101)	590 (sh) (90)	509 (135)	404 (132)
Pr^n	505 (207)	377 (99)	590 (sh) (90)	509 (136)	404 (131)
CH_2Cl	504 (200)	376 (88)	590 (sh) (90)	507 (131)	405 (128)
CH_2ClCH_2	505 (201)	377 (96)	590 (sh) (90)	509 (133)	404 (128)
$MeOCH_2$	504 (207)	376 (94)	590 (sh) (110)	506 (144)	405 (147)
Ph			590 (sh) (90)	509 (128)	403 (128)

[a] In 0.01 mol dm^{-3} HCl. [b] In water.

Table 3 Infrared spectral data (cm^{-1}) for $[Cr_2(\mu\text{-}OH)(\mu\text{-}RCO_2)(en)_4]^{4+}$, $[(nta)Cr(\mu\text{-}OH)(\mu\text{-}RCO_2)Cr(en)_2]^+$ and $Na(O_2CR)$ in the CO stretching region *

	$[Cr_2(\mu\text{-}OH)(\mu\text{-}RCO_2)(en)_4]^{4+}$			$[(nta)Cr(\mu\text{-}OH)(\mu\text{-}RCO_2)Cr(en)_2]^+$			$Na(O_2CR)$		
	$\nu_{asym}(CO)$	$\nu_{sym}(CO)$	$\Delta\nu(CO)$	$\nu_{asym}(CO)$	$\nu_{sym}(CO)$	$\Delta\nu(CO)$	$\nu_{asym}(CO)$	$\nu_{sym}(CO)$	$\Delta(CO)$
R = H	1572	1380	192	1568	1380	188	1590	1355	253
Me	1550	1422	128	1555	1420	135	1578	1425	153
Et	1540	1445	95	1545	1438	107	1553	1421	132
Pr^n	1536	1455	81	1540	1453	87	1558	1420	138
CH_2Cl	1598	1443	155	1592	1445	145	1610	1445	145
CH_2ClCH_2	1555	1455	100	1554	1458	96	1560	1420	140
$MeOCH_2$	1575	1460	115	1568	1460	108	1613	1422	191
Ph				1540	1425	115	1540	1425	115

* On KBr pellets.

ligand to form structure **a** rather than **b**. The stereochemical configuration of **a** is analogous to that in the only isomer obtained for $K_2[(nta)Cr(\mu\text{-}OH)(\mu\text{-}MeCO_2)Cr(nta)] \cdot 4H_2O$[12] and $[(tren)Cr(\mu\text{-}OH)(\mu\text{-}CO_3)Cr(tren)][ClO_4]_3 \cdot 4H_2O$,[13] for which X-ray analysis revealed that the oxygen atom of the μ-carboxylate or μ-carbonate ligand is located *cis* to the tertiary amine nitrogen in the nta or tren [tris(2-aminoethyl)-amine] ligand. These facts suggest that the configuration in structure **a** results in less steric congestion between the glycinate ring chelate in the nta ligand and the en chelate than that in **b**.

Kinetics of Base Hydrolysis of $[Cr_2(\mu\text{-}OH)(\mu\text{-}RCO_2)(en)_4]^{4+}$. —The colour of aqueous solutions of $[Cr_2(\mu\text{-}OH)(\mu\text{-}RCO_2)(en)_4]^{4+}$ changed rapidly from red to blue upon addition of hydroxide ion. This is due to deprotonation of the hydroxo bridge as reported by Springborg and Toftlund.[4] The deprotonation rate was too fast to follow even by the stopped-flow method. After deprotonation the UV/VIS spectra of the blue complex having absorption maxima at 580, 450 and 363 nm changed with time. Isosbestic points were observed at 385, 430 and 558 nm in the early phase of the reaction as shown in Fig. 1, but they disappeared as the reaction proceeded. The absorbance at 363 nm decreased up to *ca.* 90 min, then disappeared and a constant value of A_{inf} was attained. On the other hand, the absorbance at 527 nm initially increased for *ca.* 200 s, then decreased for *ca.* 90 min and thereafter remained unchanged. These spectral changes are ascribed to the first and second stages of the overall reaction. The SP-Sephadex column chromatography at 5 and 60 min during the base hydrolysis showed the existence of a tri- and a uni-positive complex ion in the reaction solution (see Experimental section). The amounts of the tri- and the uni-positive complexes decreased and increased, respectively, between the two times. They are identified as dinuclear $[(en)_2(HO)Cr(\mu\text{-}OH)Cr(OH)(en)_2]^{3+}$ and mononuclear *cis*-$[Cr(OH)_2(en)_2]^+$ not only by the UV/VIS spectra,[18] but also by the ^2H NMR spectra of the μ-CD_3CO_2 complex. The ^2H NMR behaviour of CD_3CO_2 co-ordinated to

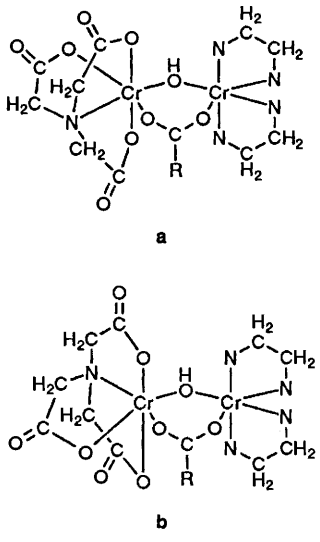

a

b

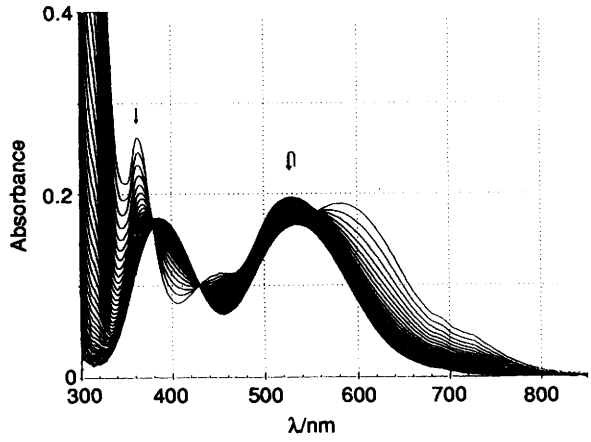

Fig. 1 Absorption spectral changes of $[Cr_2(\mu\text{-}OH)(\mu\text{-}MeCO_2)(en)_4]^{4+}$ solution (initially 3 mmol dm^{-3}) over 2 h after adding NaOH aqueous solution ([OH] = 0.5 mol dm^{-3}) at 25 °C and I = 0.5 mol dm^{-3} ($NaClO_4$). Total scanning time 90 min, time interval between scans 90 s

chromium(III) makes it possible to distinguish an uncoordinated from a co-ordinated or a monodentate from a bridging ligand. The signals for the monodentate acetate ligand appear at about δ 20.[12,19] On the other hand, bridging acetate ligands exhibit a signal ranging in chemical shift from δ 58 to 41.[12,19] Before addition of hydroxide ion, only one ^2H NMR signal was observed at δ 56 as in Fig. 2(*a*). This is assignable to the bridging deuteriated acetate ligand in $[Cr_2(\mu\text{-}OH)(\mu\text{-}CD_3CO_2)(en)_4]^{4+}$. When hydroxide ion was added three signals appeared at δ 39.0, 17.8 and 3.0 [Fig. 2(*b*)]. Among them, the intensity at δ 3.0 increased with time and was almost unchanged after about 40 min. This signal is due to free uncoordinated CD_3CO_2 ion in view of the chemical shift. The remaining two signals at δ 39.0 and 17.8 decreased with time and finally disappeared. Thus, that at δ 17.8 is due to monodentate CD_3CO_2 ligand in $[(en)_2(HO)Cr(\mu\text{-}OH)Cr(CD_3CO_2)(en)_2]^{3+}$, the amount of which is small judging from the intensity. The other one at δ 39.0 is ascribed to the bridging acetate ligand in deprotonated $[Cr_2(\mu\text{-}O)(\mu\text{-}CD_3CO_2)(en)_4]^{3+}$. The ^2H NMR spectra showed complete disappearance of the co-ordinated CD_3CO_2 signal and the appearance of free CD_3CO_2 in the acetato bridge-cleavage reaction. The NMR behaviour is in accord with the chromatographic observation that the deprotonated μ-oxo complex changed to $[(en)_2(HO)Cr(\mu\text{-}OH)Cr(OH)(en)_2]^{3+}$ in the early phase of the reaction, and that a mononuclear complex containing monodentate CD_3CO_2 like $[Cr(OH)(CD_3CO_2)(en)_2]^+$ was not formed.

From these experimental results, the first-stage reaction involves an acetato bridge cleavage giving a mono-μ-OH complex as Springborg and Toftlund[4] proposed. The second-stage reaction is decomposition of the dinuclear complex. The rate-determining steps are the first- and second-stage reactions. Almost the same absorption spectral changes were observed for all the μ-carboxylato complexes as well as the μ-acetato complex. In addition, column chromatography for all the μ-carboxylato complexes gave two bands corresponding to $[(en)_2(HO)Cr(\mu\text{-}OH)Cr(OH)(en)_2]^{3+}$ and *cis*-$[Cr(OH)_2(en)_2]^+$. Accordingly, the reaction mechanism for the μ-carboxylato complexes is the same as that for the μ-acetato complex. This evidence led us to propose the reaction mechanism in Scheme 1 for the μ-carboxylato en complexes.

The apparent rate constants (Table 4) for the first and second stages (k_{1obs} and k_{2obs}) in Scheme 1 [steps (ii) and (iv)] were obtained by monitoring the decreasing absorbance at 363 and 527 nm (arrows in Fig. 1), respectively, according to equation (2). The first stage was monitored at 363 nm, where the influence from the second stage is not present. The second stage can be monitored at 527 nm without interference from the first.

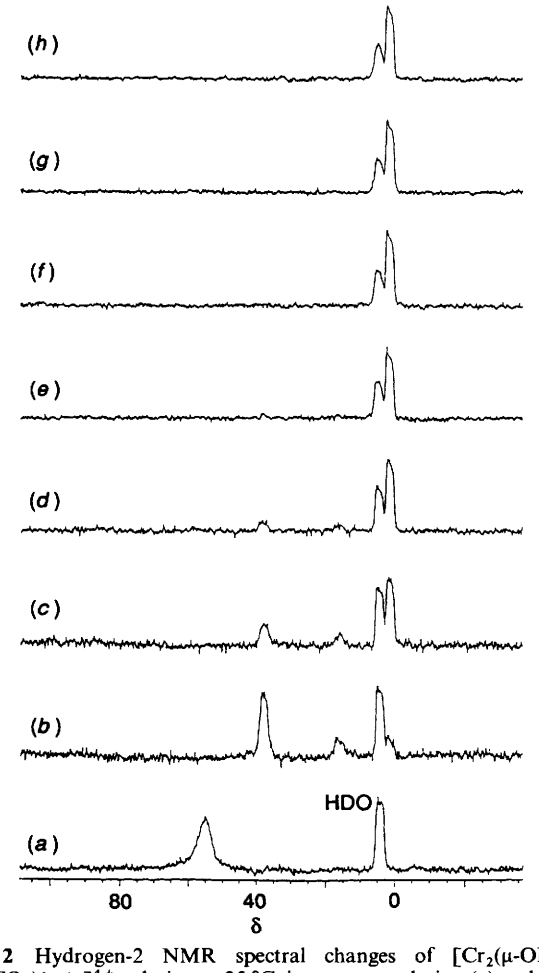

Fig. 2 Hydrogen-2 NMR spectral changes of $[Cr_2(\mu\text{-}OH)(\mu\text{-}CD_3CO_2)(en)_4]^{4+}$ solution at 25 °C: in aqueous solution (*a*) and 5 (*b*), 10 (*c*), 15 (*d*), 20 (*e*), 30 (*f*), 40 (*g*) and 50 min (*h*) after adding NaOH aqueous solution

For the monodentate carboxylate ligand-dissociation reaction in Scheme 1(iii), the rate constant (k_d) could not be estimated in this experiment, since the corresponding UV/VIS absorption spectral change was not detected, probably because of the small amount of $[(en)_2(HO)Cr(\mu\text{-}OH)Cr(CD_3CO_2)(en)_2]^{3+}$ as observed from the NMR spectra (see above).

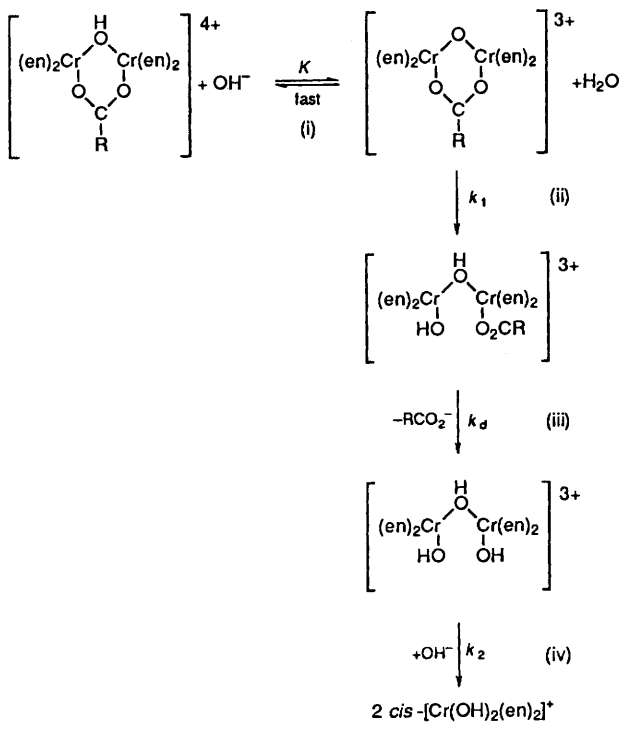

Scheme 1

The half-lives estimated from the k_{1obs} values for the μ-acetato- and μ-formato complexes have a similar order of magnitude ($t_{\frac{1}{2}} \approx 6$ min and 1 s, respectively) to those for these complexes reported by Springborg and Toftlund.[4] A hydroxide-ion concentration dependence was observed for the apparent rate constant k_{1obs} of the first stage, but not for the second.

Taking into account the acid–base equilibrium of $[Cr_2(\mu\text{-}OH)(\mu\text{-}MeCO_2)(en)_4]^{4+}$ as shown in Scheme 1 (i), the pseudo-first-order constant k_{1obs} is given by equation (4) where K and

$$k_{1obs} = \frac{K[OH^-]}{1 + K[OH^-]} \cdot k_1 \qquad (4)$$

$[OH^-]$ are the equilibrium constant for the reaction in Scheme 1 (i) and the hydroxide-ion concentration, respectively. The reaction rate constant k_1 and K were satisfactorily obtained by non-linear least-squares fits of k_{1obs} to $[OH^-]$. The values of k_1, k_2($= k_{2obs}$) and K are summarized in Table 5.

From the equilibrium constant K the acid strengths [$pK_a = -\log(KK_w)$] of the bridging hydroxide ligand can be calculated. These are also collected in Table 5. For the μ-$MeCO_2$ complex, the pK_a value (11.9) agrees with the estimated value of Springborg and Toftlund.[4] The first-stage rate constants k_1 varied from 2.85 to 7.84 × 10^{-4} s^{-1} with variation of the carboxylate in $[Cr_2(\mu\text{-}OH)(\mu\text{-}RCO_2)(en)_4]^{4+}$. Springborg and Toftlund[4] concluded that the carboxylato bridge-cleavage reaction becomes plausibly slower as the acid strength (pK_a') of the corresponding carboxylic acid decreases. On this basis, the reaction rate (k_1) of the μ-formato complex is supposed to be slower than that of the μ-monochloroacetato and μ-methoxyacetato ones. However, the k_1 value for the former complex is found to be larger by one or two orders of magnitude than those of the last two. These data cannot be accounted for only by the acidity of the carboxylates in the bridging unit. This subject will be discussed later in detail on the basis of the substituent effect. The values of k_2 are almost the same for all the complexes. Since the rate-determining step in the second stage is decomposition of the complex $[(en)_2(HO)Cr(\mu\text{-}OH)Cr(OH)(en)_2]^{3+}$ to the mononuclear complex, it is reasonable that the k_2 value of each complex is independent of the substituent group R of the μ-RCO_2^- complexes.

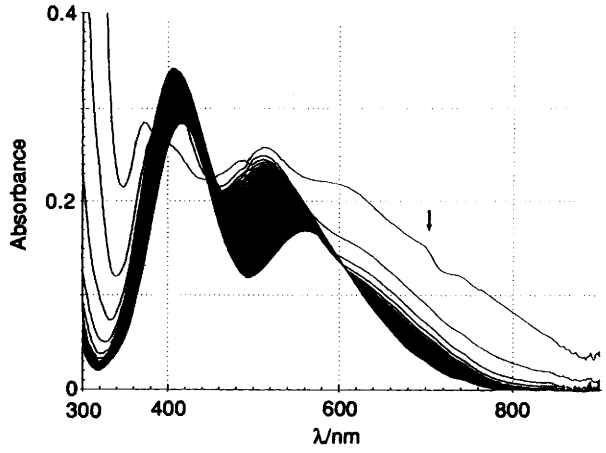

Fig. 3 Absorption spectral changes of $[(nta)Cr(\mu\text{-}OH)(\mu\text{-}MeCO_2)Cr(en)_2]^+$ (initially 5 mmol dm^{-3}) solution over 1 h after adding aqueous NaOH solution ([OH] = 0.5 mol dm^{-3}) at 25 °C and I = 0.5 mol dm^{-3} ($NaClO_4$). Total scanning time 60 min, time interval between scans 90 s

Kinetics of Base Hydrolysis of $[(nta)Cr(\mu\text{-}OH)(\mu\text{-}RCO_2)Cr(en)_2]^+$.—As in the case of the $[Cr_2(\mu\text{-}OH)(\mu\text{-}RCO_2)(en)_4]^{4+}$ complexes, addition of NaOH solution to aqueous solutions of the nta complexes resulted in a rapid change from reddish violet to blue. This suggests deprotonation of the hydroxo bridge in $[(nta)Cr(\mu\text{-}OH)(\mu\text{-}RCO_2)Cr(en)_2]^+$. The absorption spectra of the blue solutions showed maxima at 510 and 372 nm and an inflection at 700 nm. After deprotonation, the spectra changed with time as in Fig. 3.

On the basis of the SP-Sephadex cation and QAE-Sephadex anion column chromatography at 2 and 40 min after addition of hydroxide ion to the reaction solution, an uncharged red, a unipositive violet and a dinegative blue complex was found in the reaction solution. The amounts of the last two increased with time. These species were characterized by the ^2H NMR spectral changes of the reaction solution for the μ-CD_3CO_2 complex. A signal at δ 47.4 observed before addition of OH^- ion is assigned to $[(nta)Cr(\mu\text{-}OH)(\mu\text{-}CD_3CO_2)Cr(en)_2]^+$ [Fig. 4(*a*)]. When OH^- ion was added two signals appeared at δ 40.0 and 18.0 [Fig. 4(*b*)]. The former completely disappeared after 10 min [Fig. 4(*c*)] while the latter decreased with time and disappeared after 40 min, and a new signal at δ 20.0 appeared. The intensity of this signal then remained unchanged. Thus, the signals at δ 18.0 and 20.0 may be assigned to the monodentate co-ordinated CD_3CO_2 ligand in the μ-OH di- and mono-nuclear complexes, respectively, in view of the chemical shifts and the reaction mechanism. Moreover, formation of the stable mononuclear complex with the co-ordinated CD_3CO_2 ligand suggests a cleavage reaction at the $Cr(en)_2$ site of the carboxylato bridges. Otherwise, even if the ^2H NMR signal of the monodentate acetate could appear, it would disappear within a few minutes similarly as for $[Cr_2(\mu\text{-}OH)(\mu\text{-}CD_3CO_2)(en)_4]^{4+}$. Accordingly, the first-stage reaction of carboxylato bridge cleavage occurs at the $Cr(en)_2$ site to give the complex $[(CD_3CO_2)(nta)Cr(\mu\text{-}OH)Cr(OH)(en)_2]$ and finally *cis*-$[Cr(OH)_2(en)_2]^+$ and $[Cr(nta)(CD_3CO_2)(OH)]^{2-}$. The absorption spectral change at 700 nm reveals the two-stage reaction as shown in Fig. 3. The first- and second-stage rate constants k_{1obs} and k_{2obs} were obtained according to equations (3a)–(3c) using non-linear least-squares fits. Fig. 5 shows an example of a plot of $A(t)$ *vs.* t with the non-linear least-squares fit. The rate constants obtained are summarized in Table 4. All the carboxylato bridged complexes as well as the μ-acetato complex showed almost the same absorption spectral changes.

Table 4 Rate constants for $[Cr_2(\mu\text{-}OH)(\mu\text{-}RCO_2)(en)_4]^{4+}$ [a] and $[(nta)Cr(\mu\text{-}OH)(\mu\text{-}RCO_2)Cr(en)_2]^{+}$ [b] complexes

	$[Cr_2(\mu\text{-}OH)(\mu\text{-}RCO_2)(en)_4]^{4+}$			$[(nta)Cr(\mu\text{-}OH)(\mu\text{-}RCO_2)Cr(en)_2]^{+}$		
R	$[OH^-]$/mol dm^{-3}	k_{1obs}/s^{-1}	$10^{-4}k_{2obs}$/s^{-1}	$[OH^-]$/mol dm^{-3}	$10^{-2}k_{1obs}$/s^{-1}	$10^{-4}k_{2obs}$/s^{-1}
H	0.10	0.299(16)	3.14(6)[c]	0.05	5.80(7)	1.60(9)
	0.20	0.543(11)	3.14(5)[d]	0.50	5.85(4)	1.56(5)
	0.25	0.649(4)	3.15(6)[e]	1.00	5.94(6)	1.60(7)
	0.40	0.909(12)	3.17(4)[f]	2.00	5.95(4)	1.63(5)
CH_2Cl	0.10	0.664(2) × 10^{-1}	3.14(2)[c]	0.05	1.34(5)	1.31(4)
	0.20	0.109(4)	3.18(2)[d]	0.50	1.35(5)	1.42(2)
	0.25	0.122(2)	3.25(3)[e]	1.00	1.36(3)	1.38(1)
	0.40	0.157(5)	3.11(8)[f]	2.00	1.38(2)	1.55(6)
$MeOCH_2$	0.10	0.650(1) × 10^{-2}	3.15(6)	0.05	1.34(3)	1.59(4)
	0.25	1.05(1) × 10^{-2}	3.18(4)	0.50	1.32(1)	1.64(1)
	0.40	1.25(1) × 10^{-2}	3.17(3)	1.00	1.35(3)	1.66(2)
	0.50	1.35(2) × 10^{-2}	3.18(3)	2.00	1.35(3)	1.62(3)
CH_2ClCH_2	0.10	1.46(3) × 10^{-3}	3.13(5)	0.05	1.42(4)	1.58(2)
	0.25	1.51(2) × 10^{-3}	3.17(4)	0.50	1.40(2)	1.64(4)
	0.40	1.52(3) × 10^{-3}	3.17(4)	1.00	1.39(3)	1.60(6)
	0.50	1.53(1) × 10^{-3}	3.28(3)	2.00	1.40(2)	1.52(6)
Me	0.10	1.47(2) × 10^{-3}	3.21(8)	0.05	1.77(5)	1.62(4)
	0.25	1.53(1) × 10^{-3}	3.23(4)	0.50	1.73(5)	1.54(1)
	0.40	1.56(2) × 10^{-3}	3.24(8)	1.00	1.61(1)	1.45(4)
	0.50	1.57(1) × 10^{-3}	3.33(4)	2.00	1.65(1)	1.40(2)
Et	0.10	7.35(4) × 10^{-4}	3.21(3)	0.05	1.42(1)	1.45(2)
	0.25	8.64(4) × 10^{-4}	3.15(4)	0.50	1.40(1)	1.46(1)
	0.40	9.00(1) × 10^{-4}	3.15(6)	1.00	1.42(3)	1.46(2)
	0.50	9.20(4) × 10^{-4}	3.19(3)	2.00	1.43(4)	1.45(3)
Pr^n	0.10	6.78(2) × 10^{-4}	3.07(8)	0.05	1.54(2)	1.58(3)
	0.25	7.38(2) × 10^{-4}	3.11(1)	0.50	1.45(3)	1.58(4)
	0.40	7.55(1) × 10^{-4}	3.11(6)	1.00	1.50(4)	1.65(2)
	0.50	7.60(4) × 10^{-4}	3.07(6)	2.00	1.49(3)	1.68(4)
Ph				0.05	1.46(4)	1.45(2)
				0.50	1.50(4)	1.48(5)
				1.00	1.49(3)	1.47(4)
				2.00	1.49(5)	1.55(4)

[a] I = 0.5 mol dm^{-3} $NaClO_4$ at 25 °C. [b] I = 2.0 mol dm^{-3} $NaClO_4$ at 25 °C. [c] 0.1 mol dm^{-3} $[OH^-]$. [d] 0.25 mol dm^{-3} $[OH^-]$. [e] 0.4 mol dm^{-3} $[OH^-]$. [f] 0.5 mol dm^{-3} $[OH^-]$.

Table 5 Kinetic data and substituent parameters for $[Cr_2(\mu\text{-}OH)(\mu\text{-}RCO_2)(en)_4]^{4+}$ complexes[a]

R	k_1[b]/s^{-1}	$10^{-4}k_2$[b,c]/s^{-1}	K[b,d]/dm^3 mol^{-1}	pK_a[e]	σ^*[f]	E_s[f]
H	2.85(5)	3.15(1)	1.18(2)	13.9	0.490	1.24
CH_2Cl	2.86(8) × 10^{-1}	3.17(5)	3.03(14)	13.5	1.050	−0.24
$MeOCH_2$	1.83(2) × 10^{-2}	3.17(1)	5.50(16)	13.3	0.520	−0.19
CH_2ClCH_2	1.55(1) × 10^{-3}	3.19(6)	171(9)	11.8	0.385	−0.90
Me	1.59(1) × 10^{-3}	3.25(5)	119(13)	11.9	0.000	0.00
Et	9.78(3) × 10^{-4}	3.18(3)	30.2(7)	12.5	−0.100	−0.07
Pr^n	7.84(4) × 10^{-4}	3.09(2)	63.9(4)	12.2	−0.190	−0.36

[a] I = 0.5 mol dm^{-3} with $NaClO_4$ at 25 °C. [b] Standard deviations are given in parentheses in units of the last decimal. [c] Average value. [d] Equilibrium constant in Scheme 1 (i). [e] pK_a = −log(KK_w) for μ-OH moiety. Uncertainty estimated at ±0.2 pK_a unit. [f] Ref. 20.

Table 6 Kinetic and magnetic data for $[(nta)Cr(\mu\text{-}OH)(\mu\text{-}RCO_2)Cr(en)_2]^{+}$ complexes[a]

R	$10^{-2}k_1$[b,c]/s^{-1}	$10^{-3}k_2$[b,c]/s^{-1}	$2J$[c,d]/cm^{-1}
H	5.89(6)	1.60(2)	−22.6(3)
Me	1.69(6)	1.50(8)	−20.0(2)
Pr^n	1.50(3)	1.62(4)	−20.8(3)
Ph	1.49(2)	1.49(4)	−21.1(1)
Et	1.42(1)	1.46(1)	−20.2(2)
CH_2ClCH_2	1.40(1)	1.59(4)	−21.6(1)
CH_2Cl	1.36(1)	1.42(9)	−22.5(2)
$MeOCH_2$	1.34(1)	1.63(3)	−22.0(3)

[a] I = 2 mol dm^{-3} at 25 °C. [b] Average value. [c] Standard deviations are given in parentheses in units of the last decimal. [d] $2J$ refers to the coupling constant determined from the observed susceptibility data.

Similar column chromatographic behaviour for the reaction solutions was observed for all the μ-carboxylato complexes. Therefore, the reaction mechanism for the μ-carboxylato complexes appears to be the same as that for the μ-acetato complex. From the above results, the reaction mechanism in Scheme 2 is proposed.

Scheme 2 is analogous to Scheme 1 except that one of the final products contains monodentate carboxylate ligand. For these complexes, both k_{1obs} and k_{2obs} exhibit no hydroxide-ion concentration dependence. According to equation (4), therefore, the observed k_{1obs} values equal the first-stage reaction rate constant k_1. The k_1(= k_{1obs}) and k_2 (= k_{2obs}) values are summarized in Table 6. Under these conditions, $K[OH^-] \gg 1$ holds, resulting in much larger values for K than those of the en complexes. It is noted that the acid strengths for the unipositive nta complexes are unexpectedly much higher than those for the tetrapositive en complexes.

The complexes $[(nta)Cr(\mu\text{-}OH)(\mu\text{-}RCO_2)Cr(en)_2]^{+}$ exhibit little variation of the k_1, k_2 values. The k_2 values correspond to the hydroxo bridge-cleavage reaction of mono-μ-OH complexes to the mononuclear ones. In the complex $[(RCO_2)(nta)Cr(\mu\text{-}OH)Cr(OH)(en)_2]$ there are two reaction

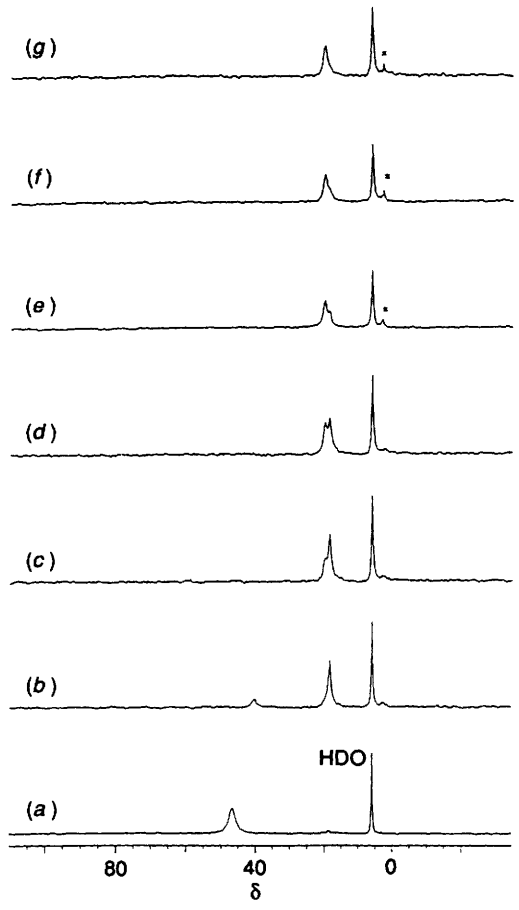

Fig. 4 Hydrogen-2 NMR spectral change of $[(nta)Cr(\mu\text{-}OH)(\mu\text{-}CD_3CO_2)Cr(en)_2]^+$ solution at 25 °C: in aqueous solution (*a*) and 5 (*b*), 10 (*c*), 15 (*d*), 20 (*e*), 30 (*f*) and 40 min (*g*) after adding NaOH aqueous solution. Asterisked signals are due to a small amount of free CD_3CO_2 anion resulting from decomposition of the reaction product

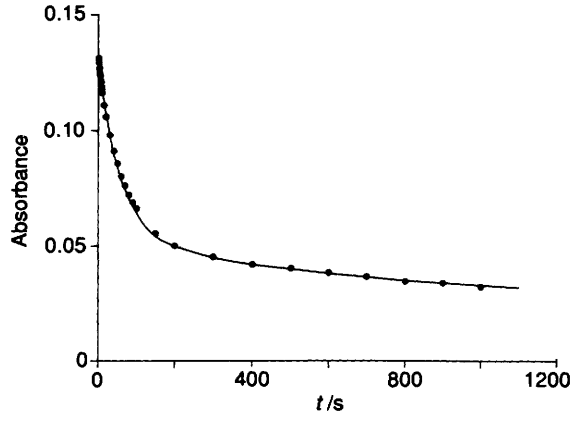

Fig. 5 Plot of absorbance *vs.* time at 700 nm for the reaction of $[(nta)Cr(\mu\text{-}OH)(\mu\text{-}MeCO_2)Cr(en)_2]^+$ (initially 5 mmol dm^{-3}) with NaOH aqueous solution ([OH] = 0.5 mol dm^{-3}) at 25 °C and I = 2 mol dm^{-3} ($NaClO_4$). The solid line is the non-linear least-squares fit

sites of the hydroxo bridge, $Cr(en)_2$ or Cr(nta). If cleavage occurs at the $Cr(en)_2$ site the k_2 values would be close to those for $[Cr_2(\mu\text{-}OH)(\mu\text{-}RCO_2)(en)_4]^{4+}$. However, the present reactions for the nta complexes are about six times faster than those of $[Cr_2(\mu\text{-}OH)(\mu\text{-}RCO_2)(en)_4]^{4+}$. In this reaction stage, therefore, the hydroxo bridge cleavage occurs at the Cr(nta) site.

Substituent Effects of Carboxylate Bridging Ligands.—In order to reveal the fundamental details of the substituent effect or the effect of the non-bridging ligands as well as the reaction mechanism, we will examine the kinetic data in terms of Taft's parameters. The reaction rate constants and the substituent effects are correlated with Taft's equation[20] (5) where σ* and E_s

$$\log(k/k_0) = \rho^*\sigma^* + \delta E_s \quad (5)$$

are the inductive and steric aliphatic substituent constants, respectively as shown in Table 5; σ* depends only on polar effects and is analogous to the Hammett substituent constant σ, E_s represents the extent of the steric effect of a substituent. The adjustable parameters ρ* and δ are constants through a reaction series and independent of the nature of the substituent groups; they give a measure of the relative susceptibility to inductive and steric requirements of the aliphatic substituents in the reaction series. The quotient k/k_0 is the relative rate of a hydrolysis reaction series for any substituent of the μ-carboxylate ligands, k_0 being the rate constant for the standard reactant (in this case the μ-acetato complexes).

This equation was applied to the k_1 values for a series of $[Cr_2(\mu\text{-}OH)(\mu\text{-}RCO_2)(en)_4]^{4+}$ complexes which vary considerably with the nature of the carboxylato bridges. Using a regression analysis for the least-squares fitting, it was found that $\log(k/k_0)$ for the rates of base hydrolysis for all seven μ-RCO_2 complexes are satisfactorily fitted with the correlation coefficient 0.993 to give the parameter values ρ* = 2.29 ± 0.20 and δ = 1.41 ± 0.13 in equation (5) (Fig. 6). This result means that the carboxylato bridge-cleavage base hydrolysis reaction for $[Cr_2(\mu\text{-}OH)(\mu\text{-}RCO_2)(en)_4]^{4+}$ is influenced by inductive and steric effects to similar extents. The reaction coefficients (ρ* and δ) of $[Cr_2(\mu\text{-}OH)(\mu\text{-}RCO_2)(en)_4]^{4+}$ are relatively large and similar to those in the methanolysis reaction of L-menthyl ester (ρ* = 2.70 and δ = 1.30).[21] In accordance with the methanolysis reaction mechanism for L-menthyl ester, the carboxylic acyl carbon atom is attacked nucleophilically by OH^- followed by C–O bond cleavage as shown in Scheme 3(*a*).

The C–O bond-cleavage reaction occurred only for $[Co(NH_3)_5(CF_3CO_2)]^{2+}$ [22] and $[Cr(NH_3)_5(CF_3CO_2)]^{2+}$,[23] while the Co–O(carboxylato) bond was ruptured in the base hydrolysis reactions of $[Co(NH_3)_5(RCO_2)]^{2+}$.[24] The anomaly at the CF_3CO_2 complex could arise from the fact that the acyl carbon is significantly activated by the strong inductive CF_3 substituent as compared with the methyl group. In our experimental results for the base hydrolysis of $[Cr_2(\mu\text{-}OH)(\mu\text{-}RCO_2)(en)_4]^{4+}$ it is to be noted that C–O bond cleavage occurs in all the complexes without strong inductive substituents like CF_3. Though the base hydrolysis for the μ-trifluoroacetato

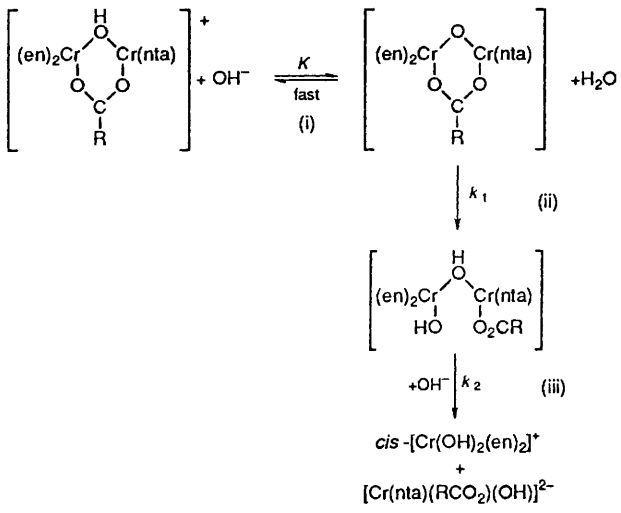

Scheme 2

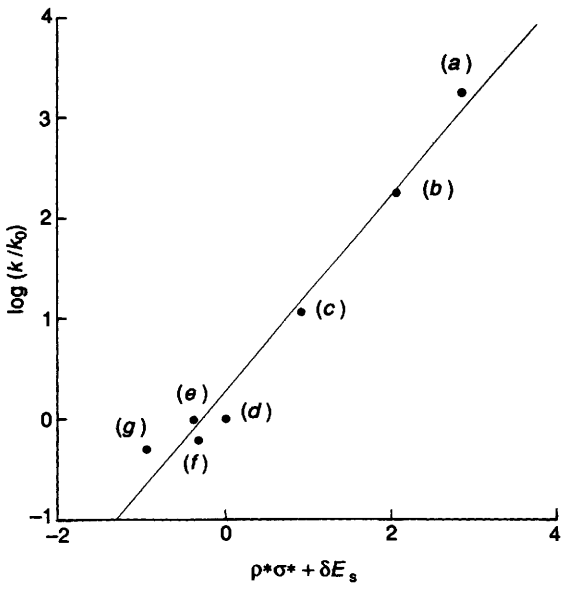

Fig. 6 Relationship between $\log(k/k_0)$ *vs.* $\rho^*\sigma^* + \delta E_s$ for carboxylato bridge-cleavage reaction constants (k_1) of $[Cr_2(\mu\text{-OH})(\mu\text{-RCO}_2)(en)_4]^{4+}$: R = H (*a*), CH_2Cl (*b*), $MeOCH_2$ (*c*), Me (*d*), CH_2ClCH_2 (*e*), Et (*f*) and Pr^n (*g*)

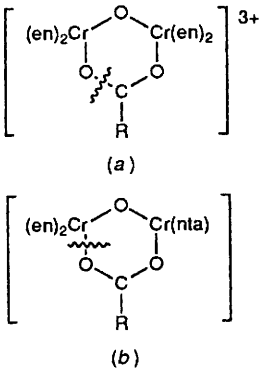

Scheme 3

complex $[Cr_2(\mu\text{-OH})(\mu\text{-CF}_3CO_2)(en)_4]^{4+}$ is assumed to involve C–O bond cleavage from a comparison with the reaction for $[Cr(NH_3)_5(CF_3CO_2)]^{2+}$,[5a] it is plausible that C–O bond rupture in the $(\mu\text{-OH})(\mu\text{-RCO}_2)$ dinuclear complexes is ascribed to acyl carbon activation due to the bidentate bridging ligation of the carboxylates rather than to the strong inductive effect of the CF_3 group.

For $[(nta)Cr(\mu\text{-OH})(\mu\text{-RCO}_2)Cr(en)_2]^+$, the k_1 values also varied with the type of carboxylato bridge (5.89×10^{-2} to 1.34×10^{-2} s^{-1}). The range is smaller than that of $[Cr_2(\mu\text{-OH})(\mu\text{-RCO}_2)(en)_4]^{4+}$. In the same manner as for the en complexes, the least-squares fitting of the relationship between the reaction rate constants and the substituent effect in equation (5) gives the values $\rho^* = 0.01 \pm 0.11$ and $\delta = 0.32 \pm 0.08$ with the correlation coefficient 0.905 as shown in Fig. 7.

For the nta complexes, unlike the en complexes, the carboxylato bridge-cleavage base hydrolysis reaction is influenced mainly by steric effects and much less by inductive ones, though the estimated uncertainty for ρ^* is rather larger than the value itself. The susceptibility to steric effects is smaller by about one fourth compared with that of the en complexes. Thus, cleavage occurs in the Cr–O (carboxylato oxygen) bond at the $Cr(en)_2$ site remote from the substituent group as Scheme 3(*b*).

From the above examinations of the kinetics for the μ-carboxylato complexes, the difference in reaction mechanisms

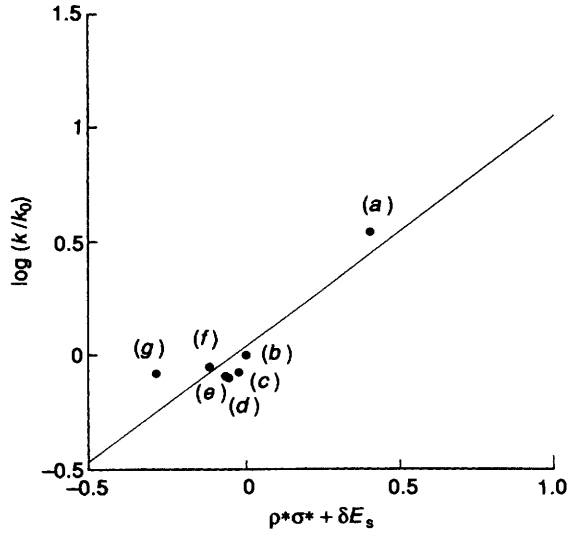

Fig. 7 Relationship between $\log(k/k_0)$ *vs.* $\rho^*\sigma^* + \delta E_s$ for carboxylato bridge-cleavage reaction constants (k_1) of $[(nta)Cr(\mu\text{-OH})(\mu\text{-RCO}_2)\text{-}Cr(en)_2]^+$: R = H (*a*), Me (*b*), Et (*c*), $MeOCH_2$ (*d*), CH_2Cl (*e*), Pr^n (*f*) or CH_2ClCH_2 (*g*)

between the en and nta complexes may be ascribed to the kinetic lability resulting from the relative charge imbalance among the acyl carbon, $Cr(en)_2$ and Cr(nta) sites, not to the intrinsic difference in the thermodynamic instability or the coordination bond (ligand-field) properties between the $(en)_2$-Cr–O and (nta)Cr–O bonds, in agreement with the similarity in the ligand-field absorption maxima as well as the magnetic interaction ($2J$) for these complexes. This is the first example of differentiating the base-hydrolysis reaction mechanisms by means of non-bridging ligands in dinuclear complexes.

References

1 M. Nakahanada, T. Fujihara, A. Fuyuhiro and S. Kaizaki, *Inorg. Chem.*, 1992, **31**, 1315.
2 B. G. Gafford, R. E. Marsh, W. P. Schaefer, J. H. Zhang, C. J. O'Connor and R. A. Holwerda, *Inorg. Chem.*, 1990, **29**, 4652.
3 (*a*) T. F. Tekut, C. J. O'Connor and R. A. Holwerda, *Inorg. Chim. Acta*, 1993, **214**, 145; (*b*) T. F. Tekut and R. A. Holwerda, *Inorg. Chem.*, 1994, **33**, 5254.
4 J. Springborg and H. Toftlund, *Acta Chem. Scand., Ser. A*, 1979, **33**, 31.
5 (*a*) J. Springborg, *Acta Chem. Scand.*, 1992, **46**, 1047; (*b*) K. Kaas and J. Springborg, *Acta Chem. Scand., Ser. A*, 1986, **40**, 515.
6 T. Fujihara and S. Kaizaki, *J. Chem. Soc., Dalton Trans.*, 1993, 2521.
7 T. Fujihara, A. Fuyuhiro and S. Kaizaki, preceding paper.
8 P. Andersen, *Coord. Chem. Rev.*, 1989, **94**, 47; J. Springborg, *Adv. Inorg. Chem.*, 1988, **32**, 55.
9 T. F. Tekut and R. A. Holwerda, *Inorg. Chem.*, 1993, **32**, 3196.
10 H. Toftlund, O. Simonsen and E. Pedersen, *Acta Chem. Scand.*, 1990, **44**, 676.
11 K. Wieghardt, M. Guttmann and D. Z. Ventur, *Z. Anorg. Allg. Chem.*, 1985, **527**, 33; P. Chaudhuri, M. Winter, H.-J. Küppers, K. Wieghardt, B. Nuber and J. Weiss, *Inorg. Chem.*, 1987, **26**, 3302; L. L. Martin, K. Wieghardt, G. Blondin, J.-J. Girerd, B. Nuber and J. Weiss, *J. Chem. Soc., Chem. Commun.*, 1990, 1767.
12 C. A. Green, N. Koine, J. I. Legg and R. D. Willett, *Inorg. Chim. Acta*, 1990, **176**, 87.
13 L. Spiccia, G. D. Fallon, A. Markiewicz, K. S. Murray and H. Riesen, *Inorg. Chem.*, 1992, **31**, 1066.
14 E. Pedersen, *Acta Chem. Scand.*, 1970, **24**, 3362.
15 N. Koine, R. J. Bianchini and J. I. Legg, *Inorg. Chem.*, 1986, **25**, 2835.
16 M. Nakahanada, K. Ino and S. Kaizaki, *J. Chem. Soc., Dalton Trans.*, 1993, 3681.
17 G. B. Deacon and R. J. Phillips, *Coord. Chem. Rev.*, 1980, **33**, 227.

18 J. Springborg and H. Toftlund, *Acta Chem. Scand., Ser. A*, 1976, **30**, 171.
19 J. E. Tackett, *Appl. Spectrosc.*, 1989, **43**, 490.
20 R. W. Taft, jun., *Steric Effects in Organic Chemistry*, ed. M. S. Newman, Wiley, New York, 1956, ch. 13.
21 W. A. Pavelich and R. W. Taft, jun., *J. Am. Chem. Soc.*, 1957, **79**, 4935.
22 R. B. Jordan and H. Taube, *J. Am. Chem. Soc.*, 1964, **86**, 3890.
23 R. Davies, G. B. Evans and R. B. Jordan, *Inorg. Chem.*, 1969, **8**, 2025.
24 F. Basolo, J. G. Bergmann and R. G. Pearson, *J. Phys. Chem.*, 1952, **56**, 22.

Received 16*th November* 1994; *Paper* 4/06989G